

RAM

● ROBOTICS
AND
MECHATRONICS

Re-design of the PIRATE robot

Y.M. Mirwani

BSC ASSIGNMENT

Committee:

dr. ir. E. Dertien
N. Botteghi, MSc
dr. ir. R.G.K.M. Aarts

January, 2020

001RaM2020
Robotics and Mechatronics
EEMathCS
University of Twente
P.O. Box 217
7500 AE Enschede
The Netherlands

Summary

This bachelor assignment contributes to the current Smart Tooling project led by Stramigioli and Botteghi (2018). The main focus of the Smart Tooling project focuses on the automation in the process industry i.e. making maintenance safer, cheaper, cleaner, and more efficient by developing new robot prototypes and tools. Robot technology is an important development in many industries, but because it is relatively new there are some uncertainties.

The main goal of the project is to create an autonomous pipe inspection robot for industrial petrochemical plants. This project consists of the design and testing of a new prototype for the pipe inspection robot. Different prototyping techniques are used in a number of design iterations in order to investigate the new innovative designs, resulting in a mock-up with internal gears in all wheels and an improved bending mechanism that is made using procedures such as laser-cutting and 3-D printing by combining parts such as wheels, gears, motors, and plates. The new pirate has an absolute compatible design with identical modules. Moreover, the new electronic infrastructure used in this prototype is suggested in order to overcome the limitations of the previous prototypes. This design does contain tests with a single V-shaped module to prove that the new design does meet the user specifications compared to the previous prototypes. The new design is highly modular using five modules of which two modules are based on. The limits were investigated during the process of building, and this makes the design a very iterative process and provides good insight in the robot. Furthermore, the development time is reduced significantly from four months to just one day.

Preface

I would like to thank my family, friends, and the PIRATE team, without whom this would have not been possible. Thank you for encouraging me throughout my study, believing in me and above all the opportunities I had. To my roommates, for all your great advice and help. From RAM, special thanks to Sander Smits. I really appreciate all the time you spent explaining me about the design procedures and all your patience with the laser-cutting and 3D-printing that greatly assisted the study. Without this expertise, this wouldn't have been possible. To my supervisor, Nicolo Botteghi, for all his support, advice, inspiration and guidance. His advice was very helpful at the time that I really needed it. To Jolanda, for calming me down when I went to see her for advice.

Contents

1	Introduction	1
1.1	Problem Context	1
1.2	PIRATE project	1
1.3	Previous Work	1
1.4	Project Goal	1
1.5	Outline	2
2	Background	3
2.1	The Dutch gas network	3
2.2	Previous Prototypes	3
2.3	Components	5
2.4	Low budget prototyping	5
2.5	Additive and Subtractive manufacturing	5
3	Analysis	6
3.1	Approach for the Redesign	6
3.2	In-wheel module	7
3.3	Bending module	8
3.4	Bearing load	10
4	Design	12
4.1	Modular Design	12
4.2	Motor CAD models	12
4.3	Modules Design	12
4.4	V-shape tractor: 3 modules	15
5	Implementation and Testing	16
5.1	Final V-shaped model	16
5.2	Control	16
5.3	Testing	17
5.4	Measurement Results	20
5.5	Final model	21
5.6	Control using keyboard	21
5.7	Design	21
6	Conclusions and Recommendations	23
6.1	Conclusions	23
6.2	Recommendations	23

A Appendix 1	24
A.1 Code	24
A.2 Additional designs, circuits and graphs	24
B Appendix2	30
B.1 Designs 2D sketches	30
Bibliography	38

1 Introduction

1.1 Problem Context

Every five years, the system of industrial petrochemical plants is checked for leaks in the Netherlands. In most of the high-pressure distribution mains, passive data loggers or pipe-inspection gauges are frequently used. However, with this method, low-pressure distribution mains cannot be inspected because the pipes in this case all have a smaller diameter including different types of intersections (e.g. T-joints, bends) as mentioned in the summary [1]. Moreover, maintenance and inspection-routines become tougher and expensive to execute and with these junctions, it becomes problematic to evaluate specific parts in the low-pressure network parts. Also, since people can't fit inside these pipes, the approach for inspecting them is by using above ground methods which involve removing layers of isolation material.

1.2 PIRATE project

The primary objective of the Pipe Inspection Robot for Autonomous Exploration project (PIRATE) is to develop an autonomous robot platform for in-pipe inspection of small diameter, low pressure (metropolitan) gas distribution mains. The current RaM group is working on the autonomous inspection of industrial pipelines with the framework of 'Smart Tooling'. Smart Tooling is a project within the European program Interrreg Vlanders-Netherlands. Relative to this, the PIRATE also aims to improve automation in the development industry by achieving a safer, cheaper, and more efficient maintenance. This robot can be positioned inside the pipe to carry out an inspection, such that workers are only required to test and repair points of interests that were implemented.

1.3 Previous Work

Moreover, in modern manufacturing industries, robots in the industrial and medical sectors make use of servomotors in their designs. To avoid pipeline supports, servomotors can also be utilized to clamp the robot in order to make the system stable. Electro-mechanical modules are made with physical components such as gears and motors onto the prototype in order to make the robot function as it did before. Not only is the mechanical robot improved and simpler, but also the electronics used is more considered during the project. The new design is highly modular using several identical modules.

1.4 Project Goal

The main goal of this thesis is to design and build a new, innovative mechatronic version of the PIRATE robot using servo motors, DC motors and laser-cut parts in order to simplify the design further. Also, this includes the possibility to control the new robot and manually navigate it through pipes using electronics with the most feasible approach. Due to the increase in size of the new prototype, the outcome of this version will make the robot more adaptable to future upcoming assignments regarding measurements, testing and control with more sensors. The study will focus on the design thinking approach in order to ideate and design the robot in a compact, robust manner. Eventually, the prototype should be able to climb vertically in the pipe. There are a few objectives to start off the new prototype's aspects shown below:

- The robot should be much simpler to debug for future references.
- It should be able to move in a planar aspect/ a pipe
- The research is taken one step further i.e. trying to achieve the robot to climb vertically in a pipe.

- Able to clamp on different diameter pipes.
- Easier to control both clamping and movement
- Reliability of the material/design is also an important category
- Relative to the economic aspects of the system, the criteria, i.e. system costs, amount of space yielded, speed with which data is acquired, will be improved in this design.

1.5 Outline

The report starts off with observing the previous work of the PIRATE robot. The third chapter proceeds onto the analysis part with calculations in order to determine which motors, servomotors and gears are required. In the fourth chapter, the dimensions of the robot was inferred and put into the design of the new prototype which will be created. The fifth chapter includes the implementation and testing of the control of the robot including the results. The project report closes with the conclusions and recommendations for future work.

2 Background

2.1 The Dutch gas network

2.1.1 Theory

There is a national network of gas mains that is divided into a high-pressure network for national distribution and a low pressure network for local distribution. The low-pressure net usually occupies most of the urban areas. Therefore, this network has the highest priority regarding risks for public health and safety.

The largest risks for cause of leakage are pipes of grey cast iron and white PVC. Grey cast iron is sensitive for corrosion. Connections are being formed by rubber or polyurethane rings. Polyethylene is less sensitive for degradation in time. It is, however, sensitive for point-loads (by tools) and tension (bend, stretch).

New networks that have been created in the last decade are also well documented. Detailed information possible never existed, or tends to get lost in giant company merges, takeovers, and (computer) system changes. There is a limited amount of information available about the rough position of the existing network. The possibility exists that for certain segments no knowledge is available about material, exact position, valves, shutters, connections, etc. [Dertien (2006)]

2.1.2 Current methodology for pipe inspection

Currently, the low pressure distribution nets are only inspected by conventional leakage searching above ground. This is a labor-intensive process and does not yield any information about layout and quality of the pipe. Only leaks that can be 'smelled' are detected. The accuracy of above ground detection is roughly several meters. By (Dutch) law, every segment of the gas pipe network has to be inspected every 5 years. It is hard to determine the necessary amount of sample inspections. High pressure mains are already inspected by robotic systems. These systems are, however, hardly full grown autonomous robots, but more passive data loggers.

2.2 Previous Prototypes

2.2.1 PIRATE V1

Figure 2.1 shows a CAD drawing of the first PIRATE prototype. The model consists of two V-shapes interconnected by a rotation module. The main use of the V-shape is to take care of the propulsion of the robot. It can clamp inside of a pipe in order to create traction and also to drive in a planar direction (horizontally) through the pipes.

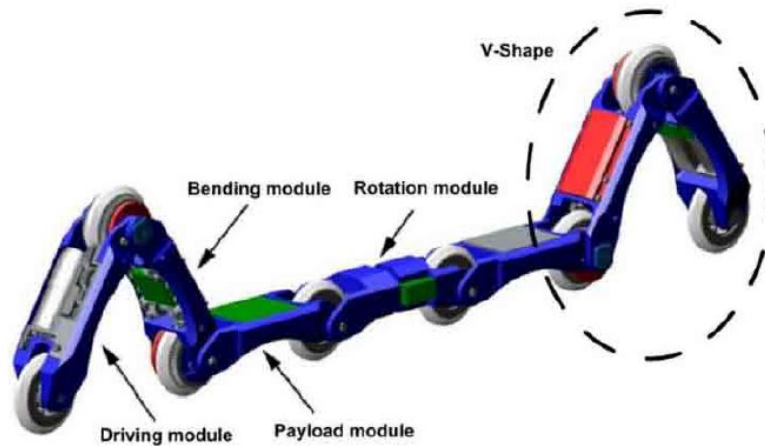


Figure 2.1: First Prototype of the PIRATE robot Pulles et al. (2008)

2.2.2 PIRATE V2

Figure 2.2 shows another version of the most recent PIRATE design, basically, an improved version of the first prototype. The original PIRATE design proposed in E. Dertien's PhD thesis[1] consisted of several modules in which this model consists of less modules than the first version but it is still divided into the 4 different types. Each module functions individually and can be combined to become a single effective unit.



Figure 2.2: Most recent version of the PIRATE robot [Pulles et al. (2008)]

- **Payload module:** Used to carry batteries, sensors, etc. for inspection in pipes.
- **Rotation module:** It is made to rotate two of the V-shapes with respect to each other. This allows the two halves of the robot to orient themselves such that bends and T-joints can be traversed. During a normal rotation procedure either the front or the back is clamped in order for the robot to be able to navigate. The rotational module also contains an Inertial Measurement Unit (IMU) sensor. This sensor is used to obtain information about the PIRATE robot's speed and acceleration.
- **Drive module:** Used to keep the modules driven in a 2-dimensional plane. Helps with the reduction of the clamping torque. Is also used to keep the motors in place for the V-shape clamping including the worm gears, spur gears, and torsional spring.
- **Bend module:** The bend module is a unit consisting of a motor for the wheels and a motor to twist the orientation with the torque that is applied.

2.3 Components

There are a few components that have to be used for this new prototype. These are related to the previous prototype which includes gears, motors, and bearings. Different types of gears are usually designed especially for laser-cutting.

Moreover, in this research perspective, a servomotor can be used for the bending module. It is simply a motor which forms a certain servomechanism. The main feature of servomotors is the ability to precisely control the position of their shaft which can be used for a clamping mechanism. As shown in figure ??, it is a closed loop system which controls its motion and final position using position feedback.

In most of the servomotors, the position feedback is generally a high precision encoder. PWM signals are mainly fed through the signal wire which can determine the movement of the servo motor. Based on these signals, the rotor of the servo motor will move in the determined position.

Both the servomotor and the DC geared motor to be found has to meet the torque, RPM, and the speed specifications. It is elaborated in more-depth in the next chapter.

2.4 Low budget prototyping

The cost of an individual robot is one of the main largest limiting factors for its collective size. The lower the robot price, the larger is the size of the collective [Rubenstein et al. (2014)]. While most robots are low cost, they still have abilities similar to other collective robots. This simplicity allows for low costs, which combined with certain scalable operations, allows for collectives much larger than what is currently available. Moreover, the robot needs enough functionality to allow it to perform a wide variety of collective behaviors, while at the same time, it must be simple enough to keep the cost low. These prospects are implemented in the design aspects and chosen in order to use low budget prototyping. The design as described uses about 5 different components shown in table A.1, which is at least 10 times less than the lowest cost of the currently used robot.

2.5 Additive and Subtractive manufacturing

Additive manufacturing growth is becoming widespread with the benefits of 3D printing in the production process. Its flexibility eases the distribution of work in the manufacturing process as it allows for mass customization in which products or components can be easily printed without the disturbance of reprogramming the software. However, it is cost-effective for small quantities. The additive manufacturing procedure will be used to make the wheels and servomounts of the robot using 3D printing. With subtractive manufacturing, laser-cutting the parts of each module will be used. This will be easier to adapt to as the plates can be used to build the module and it won't create any design restrictions.

3 Analysis

3.1 Approach for the Redesign

As mentioned in section 1.4, there are a few goals to be executed. Different techniques are used to make different versions of a robot. In this prototype, another technique and design will be created. This can be shown in several steps shown in figure 3.1. The previous robots work will be reverse engineered and then fabricated in order to build similar mechanisms. In terms of a systems engineering point of view, the system behaves similar to a V-model with relevance to both the design and testing aspects. The first step for the new prototype is to look at the requirements and specifications that basically relate to the size, performance, and price of each sub-category of the overall system. This will give enough information into how the designs should be made and whether it would be possible to start building the model or not.

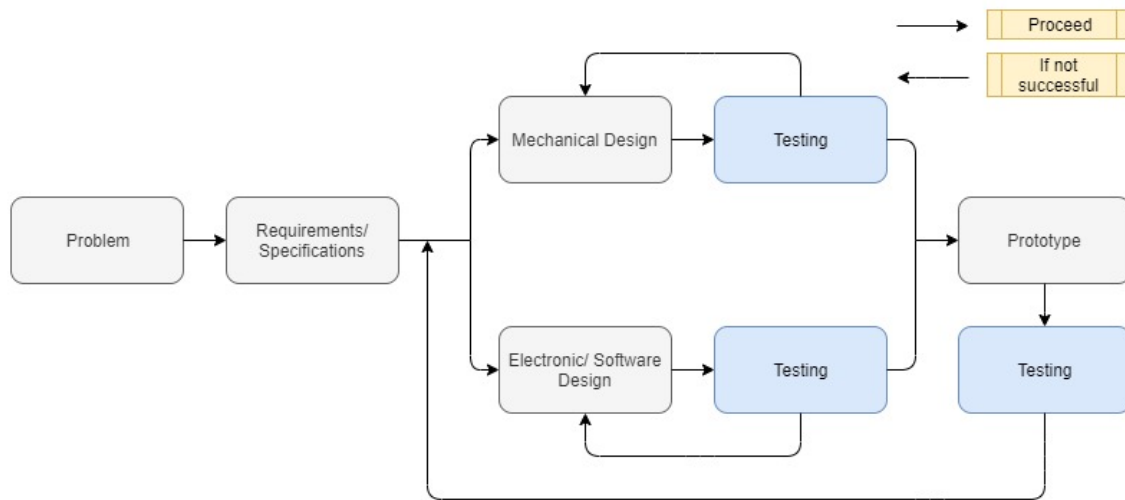


Figure 3.1: Design Trajectory mechanism

In order to purchase and work with both the servo motors and DC motors for the robot, the calculations of the clamping and motor torque is necessary. In the production phase, the design can then be implemented with the dimensions that is required to fit these motors in the necessary positions. There will then be two different modules, i.e. a bending module with servo motors and an in-wheel module with the DC motors for obtaining the final prototype. Also, for making the new design of the system, there is a selection of the parameters that will be used for the design process of the robot. In table 3.1, the properties and parameterization for the selection are shown.

Table 3.1: Selection of the parameters w.r.t previous prototype Pulles et al. (2008)

Property	Parameterization
Straight pipe [mm]	125 to 195
Inclination [°]	0 to 90
Speed variation [mm/s]	80 to 100

In addition, for the calculations, a few parameters shown in Table 3.2 are set to both its minimum and maximum values to check how the torque differs in order to choose the most suitable servomotors and DC motors.

Table 3.2: Parameters used for analysis

Parameter		Value
Mass	m	3 kg
Friction co-efficient	μ	0.3
Wheel diameter	D_w	50 mm - 70 mm
Wheel radius	r_w	25 mm - 35 mm
PIRATE speed	v	80 mm/s to 100 mm/s
Pipe diameter range	D_p	120 mm to 185 mm
Inclination	β	30, 45, 60, 90 degrees

3.2 In-wheel module

There are a few requirements for the in-wheel module such as the speed, torque, motor diameter, length, voltage, and commutation which will be determined in the upcoming sections. These are important for the robots overall movement in both horizontal and vertical pipes.

3.2.1 Motor speed

In order to fulfill the speed requirement of 80 mm/s to 100mm/s, the following formula is used referred by Braun (2016). Here, the variable N is the rotational speed in revolutions per minute, 60 is the number of seconds in a minute, and ω is the angular speed measured in radians per second (rad/s).

$$N = \frac{60}{2\pi} \omega$$

Here, the angular velocity is,

$$v = r \omega$$

$$N = \frac{60}{2\pi} \frac{v}{r_w}$$

Increasing the radius of the wheel decreases the RPM. With at least 27.28 RPM for a 70 mm wheel diameter, the motors can all move at 100mm/s which meets the requirements of the previous prototype.

3.2.2 Output torque

In order to find the total required torque to drive the PIRATE up a certain inclined slope, excluding friction losses, figure 3.2 can be used to calculate the different values. Here, the total required torque for driving the PIRATE up a slope of 30, 45, and 90 degrees, discarding friction losses can be calculated using the below formulation with gravitational force.

$$F_{tot} = mg \sin(\alpha)$$

$$T_{tot} = F_{tot} r_w$$

As shown in figure 3.4, the required torque is plotted. It can be seen that for a perpendicular pipe, the torque required is more than the torque required for other angles. This clearly means that all the motors are required to generate a maximum torque of 0.6 Nm in order to drive up perpendicular. When using 2 servomotors, the required torque to be delivered is 1.2 Nm.

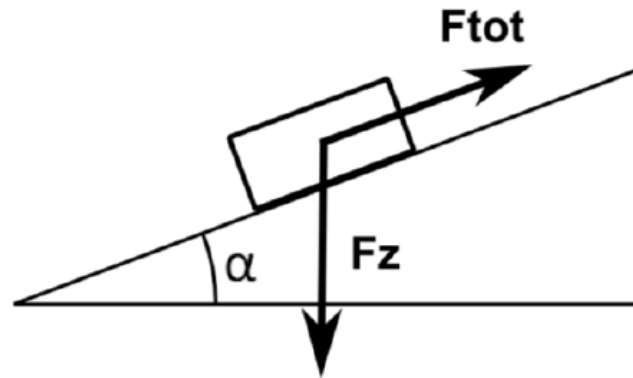


Figure 3.2: Total required Propulsion force Borgerink et al. (2016)

3.2.3 Frictional Torque

In most horizontal pipes, there is rolling resistance of the wheels in most cases. In this context, the rolling resistance is of high importance as the motor required needs to deliver high torque. In addition, if there should be more traction, then the clamping force needs to be increased which leads to a higher rolling resistance.

$$F_r = \frac{C_r T_m}{\mu r_w}$$

As mentioned in E. Dertien's report [Pulles et al. (2008)], the resulting frictional torque, with a high rolling resistance coefficient of $C_r = 0.01 - 0.015$, a motor torque of 0.5 Nm, and r_w of 55 mm, is about 5 percent of the motor torque of the wheel.

3.2.4 Motor

There will be three in-wheel drives used per V-shape. On all of the three wheels, the bending module creates traction, so it is better to use more than one module for the model. In table 3.2, the requirements for selecting the proper motor and the gearbox combination is shown. As calculated in the previous sections, table 3.3 is formulated to show the calculated values with respect to the specifications of the motor. The Hobby DC motor is chosen to be the essential

Table 3.3: Motor specifications

Requirement	Calculated values	Specifications of motor
Speed	< 34RPM	< 200RPM
Max Torque	0.41 Nm	0.6Nm
Stall torque	0.05 Nm	0.078 Nm

motor for the in-wheel drive as it meets the requirements. It is cheaper than the motors chosen from the previous project and can operate at appropriate voltages. In addition to this, due to limited resources found online, this was the best match when attached to a gear train with a ratio of 1:6 to reduce the RPM by 6 times, so that the motor moves with its nominal speed and torque.

3.3 Bending module

The bending module is to be redesigned this time with the use of servomotors. In order to choose the correct one, the nominal and maximum torque has to be calculated. The upgrade for the new redesign should meet its previous requirements, hence, it should:

- fit in the limited space available.

- provide sufficient clamping torque for both driving horizontally and vertically which also should give sufficient traction to the wheels.
- adjust the angle of clamping for different pipes

3.3.1 Required clamping torque

In order for the module to clamp inside the pipe, the nominal and maximum torque has to be known. The torque results to the normal forces of the wheel. To make it possible for the PIRATE to move in the horizontal plane, these normal forces provide the traction required. This is shown in figure 3.3.

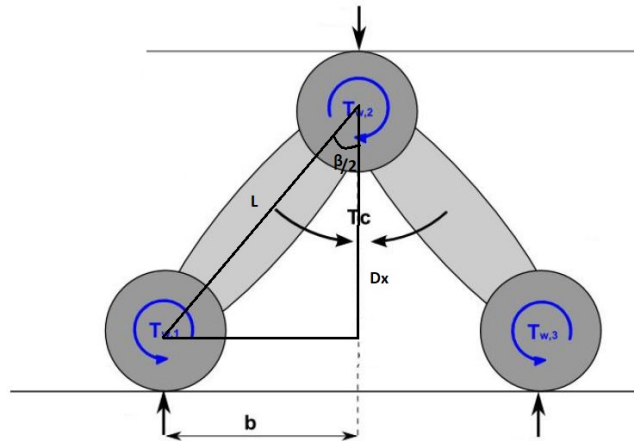


Figure 3.3: One V-shape clamped inside a pipe

The use of moving sideways through the pipe is so that it evades the dirt at the bottom of the pipe. To prevent the in-wheel module from slipping, the wheels require sufficient traction. As shown in figure 3.4, the model of the V-shape that is clamped inside the pipe is observed and the necessary traction force is proportional to the normal force which is acting on the wheel. From this figure, it can be seen that the second wheel has twice the value of the traction force

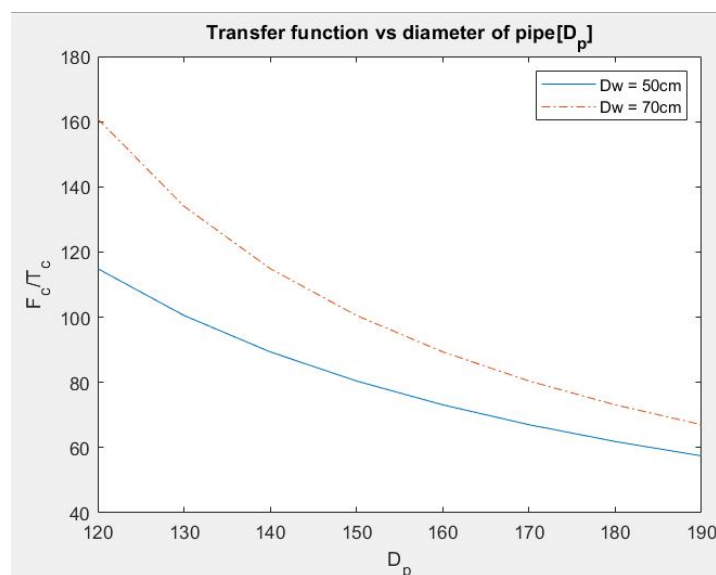


Figure 3.4: Ratio b/w clamping torque and resulting clamping force

compared to the other wheels. Hence, the clamping force required is given as follows:

$$F_n = \frac{T_c}{x}$$

In order to calculate the distance x , the length L of the module has to be determined. For now, the value of the angle between the two modules (β) that is chosen varies for different pipe diameters.

$$D_x = D_p - D_w$$

$D_w = [50, 60, 70]$ and $D_p = [120, \dots, 190]$ were the chosen values for the calculations.

In order to calculate the value of x , the length L of the module has to be determined. For now, the value of β chosen was $\beta = [30, 45, 90]$.

$$L = \frac{D_x}{\cos(\frac{\beta}{2})}$$

Hence, x can now be calculated using the formula below:

$$x = \sqrt{L^2 - D_x^2}$$

Here, the weight of the robot that has to be moved is the factor which is limited. Consider a slope α , at which the total mass of the robot is m . then the total traction force required for is equal to

$$F_{tr} = \frac{1}{2} m g \sin(\alpha)$$

In addition to this, the clamping force necessary depends on the traction force and the friction co-efficient i.e. μ given as follows,

$$F_c = \frac{F_{tr}}{\mu}$$

This results to the clamping torque using the above formula. Since the V-shape yields twice the clamping force at the wheel, the necessary torque required per joint is eventually halved. In Appendix A, table A.9 shows the values for the clamping torque calculations mentioned. As shown in figure 3.4, the variations of the diameter of the pipe and the angle of clamping is implemented with diameters of the wheel that are 50 mm and 70 mm. Choosing the pipe diameters between 125 mm and 195 mm, as it will be used to test the robot, the ratios between the length of the module and the pipe can determine the angle at which the clamping position should occur that also leads to different torques. This can also be seen in figure A.6.

Table 3.4: Minimum and maximum value of β for D_p (125mm-195mm)

Requirement	β for ($D_w = 50$ mm)	β for ($D_w = 70$ mm)
D_p (125 mm)	164.8 °	140.5 °
D_p (195 mm)	73.1 °	90 °

3.4 Bearing load

For selecting the bearing, the dimensions are determined by the amount, direction and type of load on the bearing. Depending on the type of load on the bearing in operation, the bearings are divided into two groups for research purposes Global (2017) shown below:

- Bearings loaded dynamically:
Here, the loaded bearing rotates and the selection of a suitable bearing is determined by its life due to contact fatigue of the material determined by its dynamic load rating.
- Bearings loaded statically:
In case of static loading, the bearing is loaded at standstill at very slow rotation or swinging movements determined by its static load rating.

In addition to this, the life of a rolling bearing is the number of revolutions made to the moment when the first traces of fatigue of material on rolling elements or orbital paths appear. In order to check the service life of bearings, the equation is defined below.

$$L = \left(\frac{C}{P}\right)^p$$

Here, $p = 3$ for ball bearings which will be used in this case. With the dynamic load to be $C = 22$ kg and the static load to be $P = 15$ kg, the value of L is 3.154. With this value, the life of the bearing can last for a minimum of 1 million rotations without load.

4 Design

In this chapter, the components of each module are designed. For the redesign of the PIRATE robot, during the production phase, a certain design procedure is made and divided into different parts. The design and operation of a robot requires integration of many different systems with a multi-discipline mechatronic approach. Low cost robots are identified as those robots whose cost is at low level but also the components are taken from the market. Consequently, they have the main characteristics of being of simple design, easy operation, and with limited programming capability so that generally they can be devoted to specific tasks for easy manipulations [Ceccarelli (2003)].

The process of implementation in this aspect is to first design the two different modules and then fabricate them separately, Then, it is integrated together and tested with a few experiments. The design sketches are shown in Appendix B.

4.1 Modular Design

The structure of the robot allows for a separation in each module with its specific function. The maintenance and operation of the design has a few advantages i.e. when both the electrical and mechanical interface between both the modules is well chosen, then the modules can be interchanged for maintenance and it can then be added or removed for different tasks. The concept of using plates is better for system compared to using 3D printing [Fitzner et al. (2017)]. For the increase in the manufacturability of the system, it can be achieved by consisting of modules that are made using the same identical parts. Hence, a modular design has been chosen for the robot system. The robot consists of five modules with specific functions: three modules to drive the robot and two modules to clamp the robot in the pipe.

Table 4.1: Dimensions of the Robot

Paramter	1 module	Overall robot
Length [mm]	194.48	850
Width [mm]	76.5	76.5
Height [mm]	50	50

As can be seen in figure 4.1, the robots side plate has a symmetric layout. The maximum module size is determined by the pipe diameters and obstacles which is calculated and shown in Table 4.1. At least at one of the surface planes, the size of a module cannot exceed the size of the minimal pipe diameter. There are a few other constraints other than clamping i.e. moving through sharp elbow joints and T-joints. These constraints have resulted in a curved module shape.

4.2 Motor CAD models

As shown in figure A.1, the DC geared motor CAD model is designed for the prototype. In this case, the dimensions are accurate to ± 0.5 mm. The servomotor CAD model is also shown in figure A.1. Both CAD models are used to fit and create a design from scratch for laser-cutting and 3D-printing purposes.

4.3 Modules Design

4.3.1 Wheel Module

For this module, the proposed design is shown in figure 4.2. It consists of the 3D-printed wheel and the motor integrated aside of it afterwards. In addition to this, the design basically consists



Figure 4.1: Side Design

of a gearbox pre-made from before, but also includes another set that consists of double reduction gears which will be implemented. These double reduction gears have 2 ratios i.e 1:2 for the first set of gears and 1:3 for the second set of gears which eventually becomes a 1:6 gear-set that meets the requirements of the proposed design.

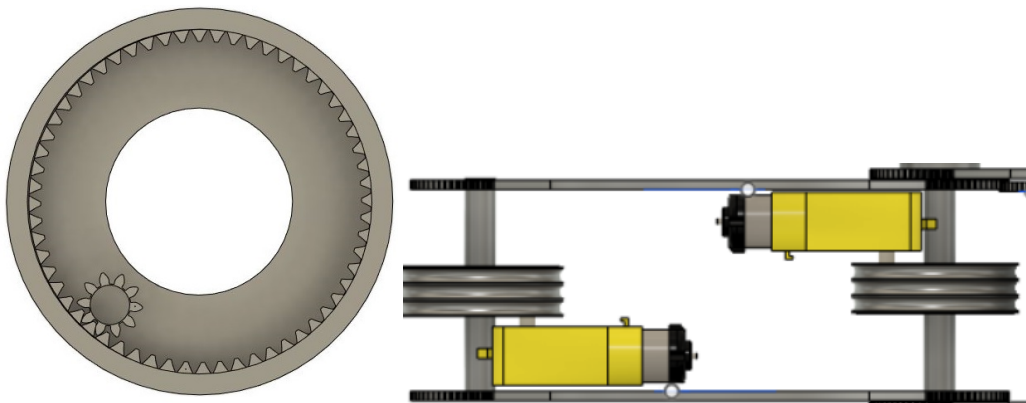


Figure 4.2: Mechanism of gears in the wheel(left) and top view of wheel module (right)

4.3.2 Bending Module

This module is an integration of the previous components and laser-cut parts. To drive sideways through a pipe, the robot always needs to exert a certain force on the wall in order to keep itself in the centre. The top view of the model is shown in figure 4.3. It can generate this

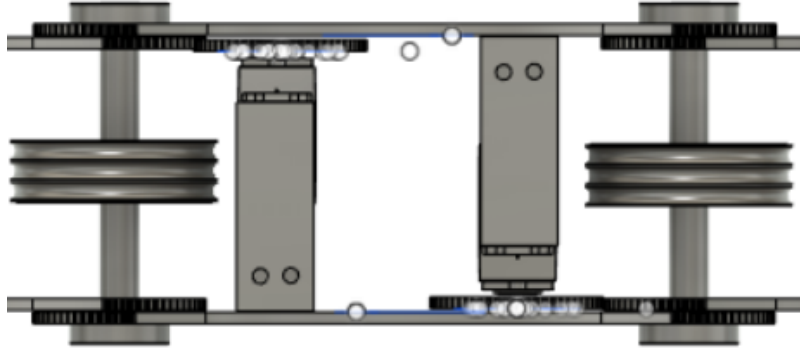


Figure 4.3: Top view of bending module

clamping force through a torque between the first two modules and the last two modules of the robot. Two servo motors with a gear connected are used to generate this clamping torque. The design shown in figure 4.4 basically shows the mounting of the servomotor with the gears in order to see how the module would be able to turn. It also shows the reliability of gears on the module as it saves space and disassembling time. In addition to this, the extra side of gears in this prototype is added in case the working part with the gears break. In this case, the gears on the side of the module are with 70 teeth. Half of this is used to turn the module at a total of 180 degrees. Using two servomotors in the same module can be advantageous as it can then handle bumps by having to adjust the control mechanism.

Servo motor Mount

The servo mount is shown in figure 4.4. This is 3D printed as the servomotor bought didn't have the exact values of what was there in the RaM lab. Hence, the laser-cutter wasn't used in this case as it would also not be that strong as the 3D printed material when the servomotor is in its maximum operation.

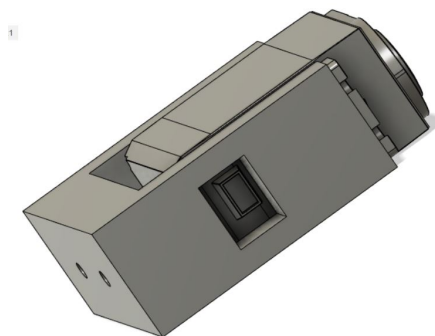


Figure 4.4: 3D printed Design for servo-mounting

Spring gear mounting

A simulation is done to check whether the spring gear can work on the mounting of the servo motor for clamping the two modules. In figure A.4, the forces acting on the spring gear is perpendicular to each other to make the gear also act as a spring. However, due to the movement in both directions, it eventually becomes not sturdy and can move on the shaft as it is made of plastic material. For testing the movements of the forces, the impact in the beginning is set to high as when the servomotor starts up, it has a fast movement. The simulation setup of the magnitudes and timings of this task is shown in figure A.8. using steps from Aasvik (2015).

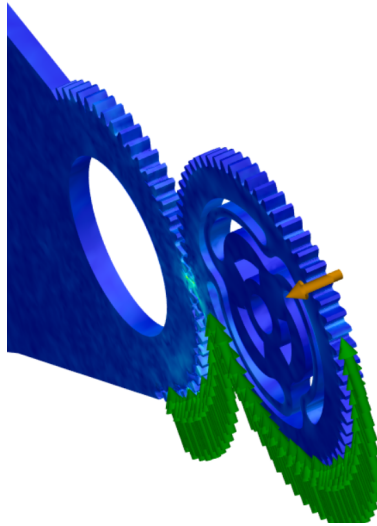


Figure 4.5: Final design

4.4 V-shape tractor: 3 modules

The V-shape tractor is the combination of the previous sections shown in figures 4.1 and 4.2. This is shown in fig 4.6 where both un-clamped and clamped is implemented.

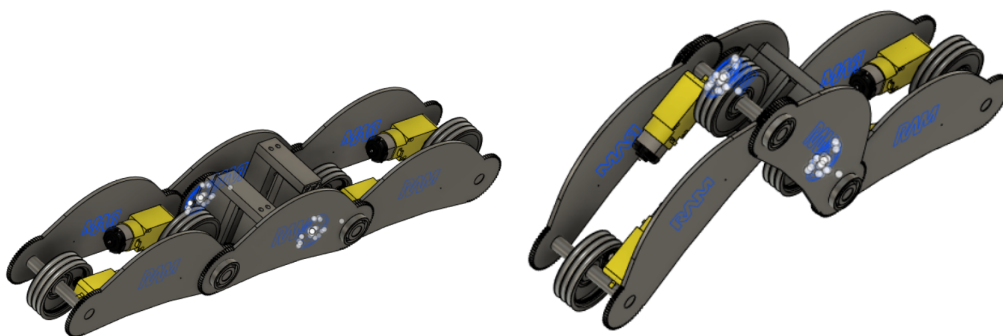


Figure 4.6: Combined module both un-clamped (left) and clamped (right)

The final design is shown in figure A.5. This model consists of the in-wheel module combined with the bending module. The screws and bolts are added in real life and not in the design as there would be some displacements made from the laser-cutter. This design was not built as the V-shape model is first implemented. It is still realised in the design process as the length and weight of the overall model is important to determine a few parameters.

5 Implementation and Testing

5.1 Final V-shaped model

In figure 5.1. the v-shaped model after the mechanical design process is finally built and the only remaining part of the production phase is the implementation and testing of the final model.

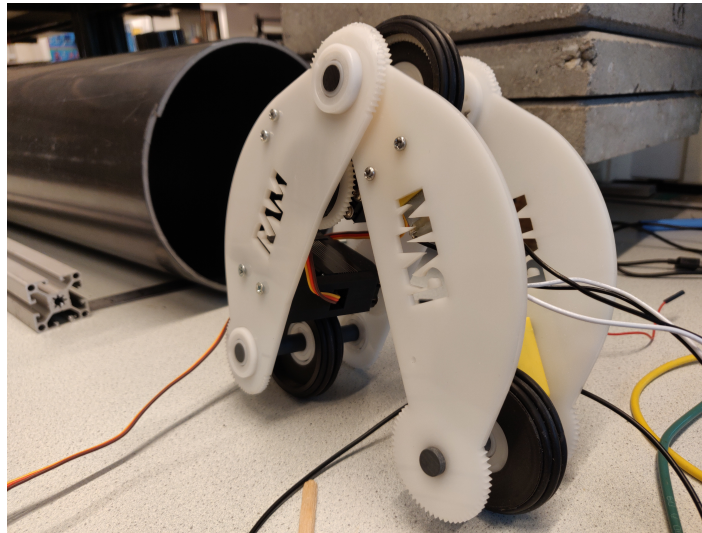


Figure 5.1: V-shaped model

5.2 Control

5.2.1 Servomotors

To control the servomotors with Arduino, a few steps were made shown below.

- Adjust angle for clamping
- Use of the button to initialize the clamp.
- Use of an extra button to reset the robot to it's initial position

When the program starts running, a counter is placed until it reads a value sent from the button. The reason for this is due to the startup current being too high for the servomotor. Shown in Appendix A is the code for clamping these servomotors. The code is done in such a way that first the user inputs a range of the clamp. After that, it checks whether the user has pressed one of the buttons, and if so, then the servo clamps till the range mentioned by the user and unclamps while the other button is pressed. This range is already measured from before so that it acts as a lookup table for the user. In addition to this, the initial start position of the servomotor will be undefined sometimes, so the servomotor initially goes to the start position of the module i.e. at 90 degrees. After that, the clamping button can be pressed to show until what position it can turn to. When the motor has rotated x degrees maximum, then it will send a message to the command window which says Max angle. To unclamp the model, the other button is pressed and it will first go to the initial position. During the measurement setup, it was observed that the increment in degrees for the first servo motor is inversely proportional to the second servo's operation.

5.2.2 DC motors

For controlling the DC motors, the L293d motor driver used is shown in Appendix A in figure A.7. The pin assignments for the connections are shown in Figure A.3. For the implementation, there are 2 buttons and 1 potentiometer. For this operation. the button is made to change the direction of the motor spin and the potentiometer is used to regulate the speed of the operation.

In addition to this, it was first implemented using MATLAB Simulink to see how to mechanism is supposed to be. Using switches in this case, the motor can spin in different directions and also can switch on and off. This is shown in figure 5.8 that describes the forward and backward mechanism using the L293d motor driver.

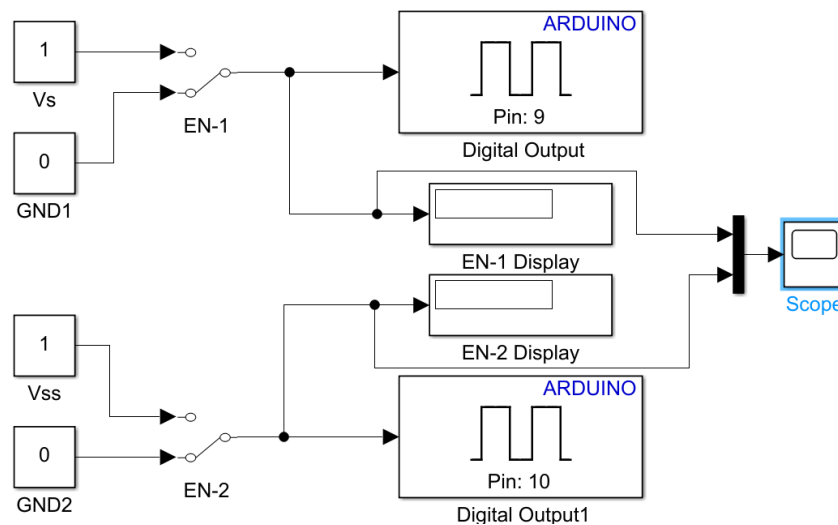


Figure 5.2: DC motor control

5.3 Testing

After the design and implementation process, the integration of both the modules is tested. Focusing on the V-shape, the following could be interesting to know:

- Clamping force/torque
- Motor output torque
- Angle between the modules

5.3.1 Clamping torque measurements

For measuring the clamping torque, the measurement setup is shown in figure 5.3 The measurement data of the mass is recorded for different intervals of clamping. Here, the relation between the clamping torque (T) and mass (m) of the model is given by:

$$T = F_n \cdot b = \frac{m \cdot g}{2} \cdot b$$

with gravitational acceleration ($g=9.81 m/s^2$) moment arm (b), axis to axis length of the module (l), diameter of the pipe (D_p) and wheel diameter ($D_w = 55mm$).

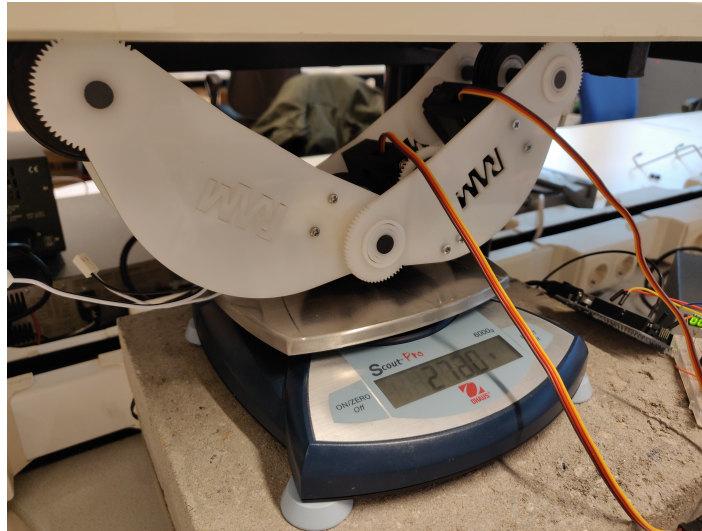


Figure 5.3: Measurement setup for clamping torque

The factor 2 is used in the formula since the measured weight is either from wheels 1 and 3 or from wheel 2 which means that twice the normal force is measured. To take gravity into

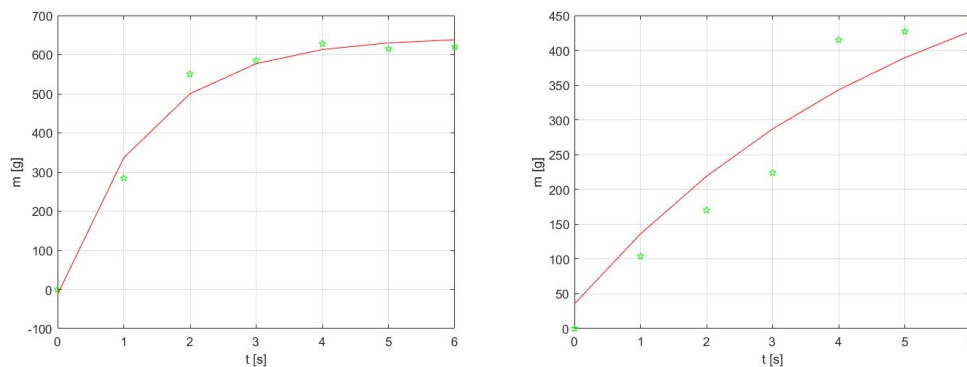


Figure 5.4: 145 mm (left) and 165 mm (right) pipe distance

account, measurements are carried out with the PIRATE horizontally flipped. In figure 5.4, for both the pipe distances, the initial value on the scale is set to 0g and the mass reaches its maximum at 620g. This is set to check how much clamping force there is, and using the formula above, the maximum torque required by the servo motor is 0.55 Nm. The servomotor does satisfy this at 4.8V already with a torque of 1.765 Nm. This indicates that the required clamping torque is met. From this, it can be seen that the mechanism performs less than expected and the servomotors can actually handle a lot more load on it. Hence, more weight can be added to the modules as the maximum torque is yet not reached.

5.3.2 DC Motor measurements

In Figure 5.5, the measurements for the DC motor are shown. The Dc motors can handle certain amount of load until it is not able to draw more current from the supply. This current increases in the case of increasing pipe inclination. This shows that at 60 degrees, the maximum load has been reached on the DC geared motor and it cannot provide enough power to drive the modules upward.

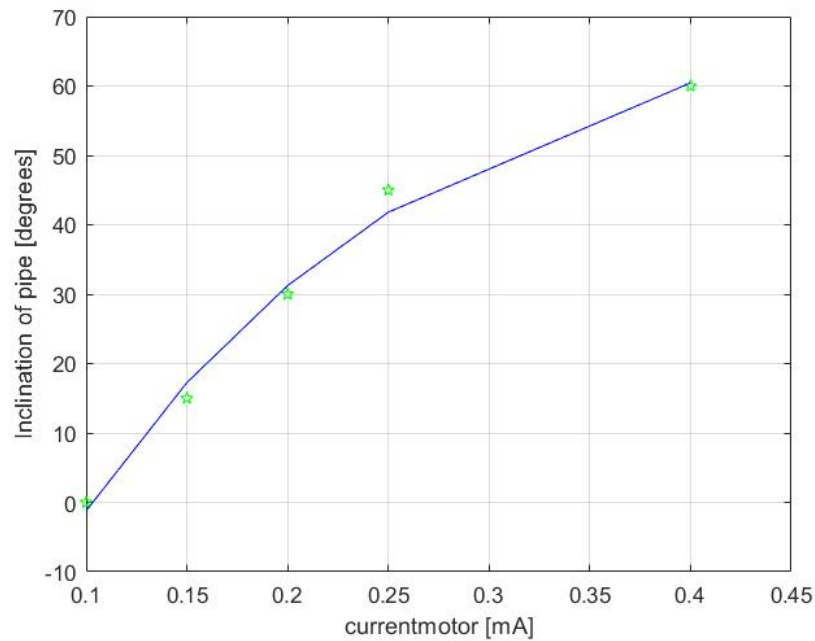


Figure 5.5: Angle of inclination of pipe vs Motor current

Angle between the modules

The angle between the two neighboring modules is used to determine the robots pose and for clamping modules, It gives information about the inner pipe diameter. In the previous prototypes, this was measured using potentiometers/ SPI angular sensor PCM made [Borgerink et al. (2016)], of which the output voltage is proportional to the angle, however, the main aim is to create a "new design" as to know how much distance between the pipes can be noticed. There

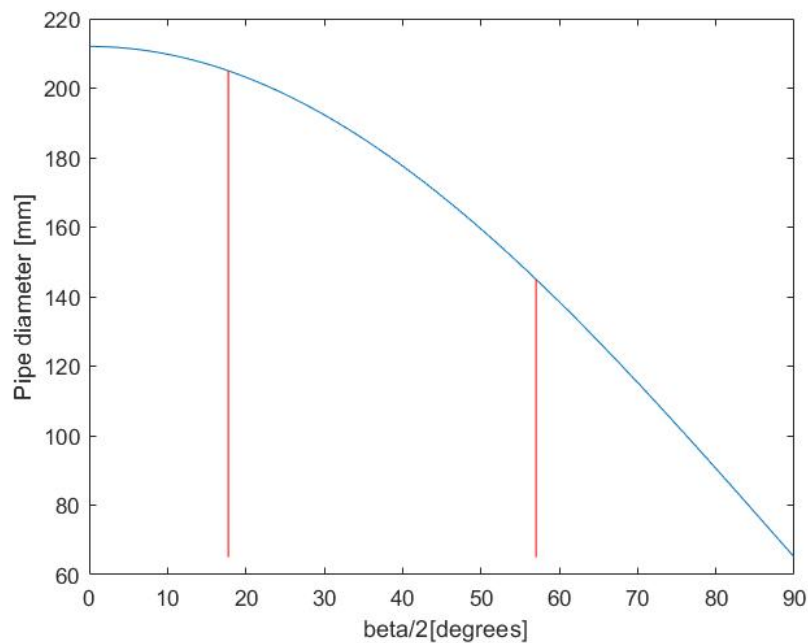


Figure 5.6: Pipe diameter vs angle β

is already an encoder in the servomotor for the angle in this case, so if the initial position is already known, then the angle of the pipes can be determined using some measures shown in figure 5.6. The blue line in the figure shows the values of the angle between the two neighboring modules for a specific diameter of the pipes, whereas the red lines show the limits to which the robot can clamp at i.e. between 145mm and 205mm pipes.

5.3.3 Further tests in 196 mm pipe

Some additional experiments were done to test in order to check if the robot meets the requirements. As shown in only figure 5.9, the robot is indeed clamped and up a 30 degrees slope. Since the results would not say much, it can be summarized below of how the robot behaved.



Figure 5.7: Measurement setup for clamping torque

- The clamping torque mechanisms indeed do work when a torque is applied, however, the wheels are not that big and does create some limitations in this prototype. This should be increased such that there is more variations in the prototype.
- The robot can also drive through the other pipes at smaller inclinations shown in figure A.2
- The robot can pull a certain amount of force when driving horizontally in a pipe; with only two wheels, as the other doesn't have traction due to the applied force.

5.4 Measurement Results

The measurements are performed in a pipe with a diameter of 196 mm and a spring scale for the clamping torque. Here the bending module is clamped inside the pipe with a clamping torque of approximately 550 mNm. With this clamp torque, the friction coefficient cannot be measured as the robot doesn't slide even when the model is vertically in the pipe.

To measure the friction coefficient, the clamp torque has to be less than 550 mNm. Here for the motor current has to be far less than 0.12 Ampere. The bending motors are less efficient at these low motor current and clamp very slowly, which is not a good solution [Borgerink et al. (2016)]. Therefore it is not convenient to measure the friction coefficient at these very low motor currents.

The tests were done with a part of the complete robot consisting of one clamping V-shape containing wires and connections. The robot has been controlled through a flat-cable using an

Arduino Uno board with additional H-bridge drivers. For every driven wheel, both forward and backward motion is possible. For the servomotor, there is already an encoder in it that is used for measuring the angle.

The figures in the above sections show measurements of the robot driving in a horizontal pipe of 196mm. When the robot starts to move, the current consumption required for the propulsion torque is constant. During the measurements, the only problem that couldn't be solved was how the clamping torque affected the motor torque.

Both test were done with an easy, smooth manual motor control keeping the motor power as low as possible. The drive motors were also set to full power after a clamping force was applied beforehand. Tests in the pipes for this case were not done as the DC motors can burn due to the high voltage.

5.5 Final model

5.6 Control using keyboard

As shown in Appendix A in Code for Final robot, the code is divided in a few parts. The use of arrays, for loops and a switch statement simplifies the code compared to the one done for the V-shaped model. An array of servos are declared in addition to the clamping and unclamping variables used for limiting the array of angles which can be changed for traction in different pipes. The ASCII table is used as there would've been more than 10 buttons made. There are 2 letters used for each servomotor and 3 letters used for the dc motor control of the keyboard. To clamp the system, an increment of the angle is written to the servo for each servo motor, and to unclamp the system, a decrement of the angle is written. The use of Boolean attributes basically writes 1s and 0s as the servo reads these values. This can also be seen here using keyboard buttons shown in figure ???. It was important to control the servomotors as the final outcome

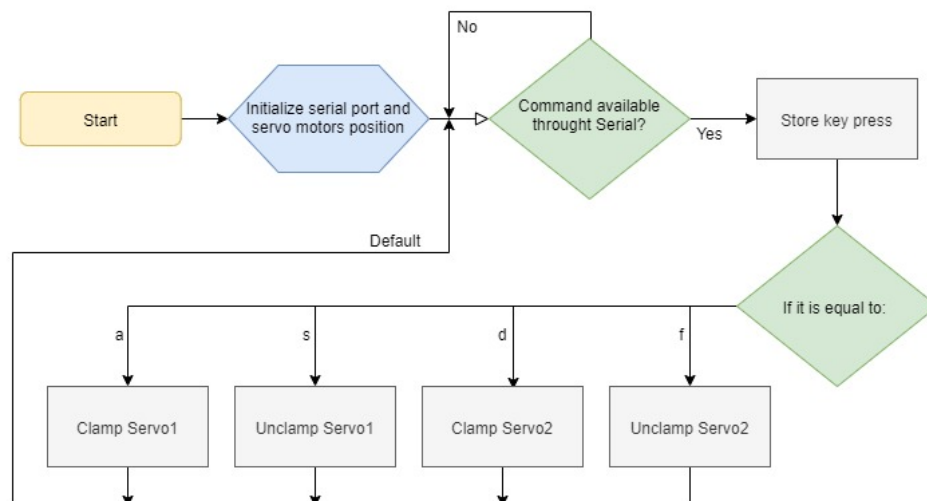


Figure 5.8: Servo motor control

of the robot moving would be noticed. This is an additional goal to the main objectives i.e. to make a cheap robot and a simplified design.

5.7 Design

The final module consists of 3 wheel modules and 2 clamping modules as shown in figure ??. There are now two V-shapes that can be clamped by the servomotors. It can clamp in order to create traction and can also drive in a planar direction inside the pipe. For this current proto-



Figure 5.9: Final version of the redesign

type, only two of the servomotors are used as it has sufficient clamping torque for the traction mechanism. Moreover, the other servo motors are also attached for future mechanisms as then, 4 of the joints of the robot can be operated.

6 Conclusions and Recommendations

6.1 Conclusions

In this bachelor project, an innovative, fully mechatronic design is developed. Not only the mechanical robot is simpler, but also the electronics of the robot is considered during the project. The prototype can clamp vertically in the biggest 196 mm pipe, but due to limitations to the DC motor it is not able to drive upward. Also, a servo motor with gears on the shaft is used in order to add compliance to the clamping mechanism.

As shown in figure A.4, the robot doesn't have a complex structure so it's simpler to debug for future preferences. From the clamping measurements, the robot was able to clamp on different diameter pipes including the 196 mm diameter pipe. It was able to move in a planar aspect and could also be controlled by moving forward and backward using the motor driver. The robot was able to clamp vertically in a pipe, however, it wasn't able to drive upwards due to insufficient motor torque. Relative to the economic aspects of the system, the criteria, i.e. system costs and amount of space yielded, is improved in this design.

The current design that is yielded using this methodology is both lightweight and low budget, since many of the multidisciplinary design choices that is necessary in mechatronics have been dealt with in rapid design iterations, such as the placement of the sensors, selection and placement of motor configuration (gearbox, sensors, size), dimensions and placement of the electronics, etc.

6.2 Recommendations

Although this prototype does meet the majority of its specifications, there is still some future work to be done before this design is fully ready. The 3D printed models proved to be very helpful during the project to gain insight and to significantly increase the development speed. However, a recommendation for the servo-mount is to make a combination of the laser-cut plates and some 3D printed material to reduce the weight and size. Using convectional techniques would be better to make the bodies from one piece or by cleverly splitting the bodies in parts from multiple pieces: making it cheaper and more compact. The final robot is unable to use the motor drivers due to the current limitation i.e. 600 mA. Each motor is able to have a stall current of about 0.8A without traction and about 1.4A with traction.

Furture recommendation for this is to control the clamping mechanism with the DC motors too as it will realize the lower limit of the current. Motor controller boards from previous prototypes can be integrated in this using more suitable motor drivers with current limiters and two separate current sensors.

The design is almost finished and it proved to be challenging to find the proper components to fit and try to make more space. As the main aim of this thesis is to build a new design, not everything can be taken into account. To know how much clamping is required is a new recommendation and elasticity with springs can be used in this prototype just like the previous one. The new PIRATE design has an all-wheel drive and therefore a sort of traction control needs to be implemented in order to generate sufficient clamping at different timings as the servomotors are quite strong already. This is completely new compared to the previous prototypes and some control strategies are implemented in this project, but not tested shown in Appendix A.

The current test pipes at the RaM lab are sufficient to do some simple test, but should also consist for the 196 mm pipe a T-joint for testing the servomotors in the robot as there is variation of current being drawn from the supply and can basically show the behaviour. The servomotor is stronger than is strictly necessary, and thereby the robot can be made more compact and compliant using even smaller servo-mounts.

A Appendix 1

A.1 Code

A.1.1 Matlab code

MAT (2019)

```

%% Measurement 1 using 145 mm distance clamp
f = @(b,x) b(1).*exp(b(2).*x)+b(3);
% Objective Function
B = fminsearch(@(b) norm(y - f(b,x)), [-200; 11; -100]);
% Estimate Parameters
figure;
plot(x, y1, 'pg');
hold on;
plot(x, f(B,x), '-r');
hold off;
grid;
xlabel('t [s]');
ylabel('m [g]');
text(27, 105, sprintf('f(x) = %.1f\cdote^{%.3f\cdotx}%.1f', B));
%% Measurement 2 using 170 mm distance clamp
f = @(b,x) b(1).*exp(b(2).*x)+b(3);
% Objective Function
B = fminsearch(@(b) norm(y - f(b,x)), [-200; 11; -100]);
% Estimate Parameters
figure;
plot(x, y2, 'pg');
hold on;
plot(x, f(B,x), '-r');
hold off;
grid;
xlabel('t [s]');
ylabel('m [g]');
text(27, 105, sprintf('f(x) = %.1f\cdote^{%.3f\cdotx}%.1f', B));
%% Measurement using dc motor
f = @(b,x) b(1).*exp(b(2).*x)+b(3); % Objective Function
B = fminsearch(@(b) norm(y - f(b,x)), [-0.6; -1; -1]);
% Estimate Parameters
figure;
plot(x, y, 'pg');
hold on;
plot(x, f(B,x), '-b');
hold off;
grid;
xlabel('currentmotor [mA]');
ylabel('Inclination of pipe [degrees]');
text(27, 105, sprintf('f(x) = %.1f\cdote^{%.3f\cdotx}%.1f', B));

```

A.2 Additional designs, circuits and graphs

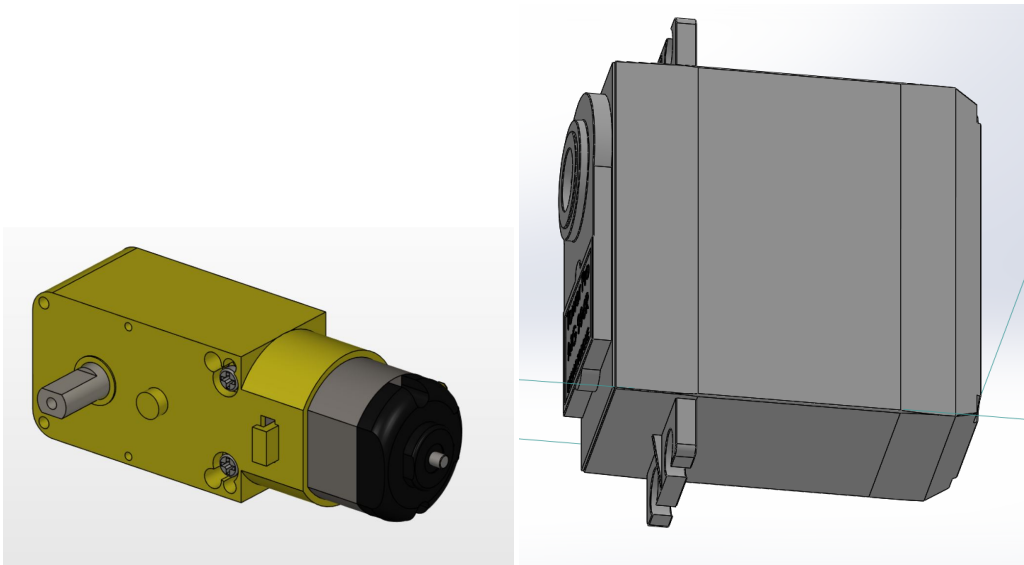


Figure A.1: CAD models of motors

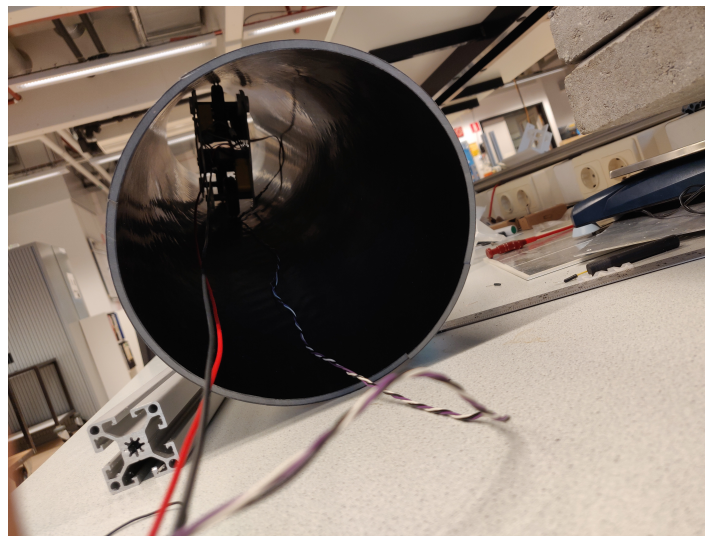


Figure A.2: Inclined pipe for testing

Table A.1: Selection of the user specifications for new prototype

Name	Type
MG958	Servomotor
Hobby DC motor	DC Geared motor
10 mm Radial Ball Bearing 26 mm OD	Bearings
Laser-cut plates	POM
3D-printed material	Carbon-fiber

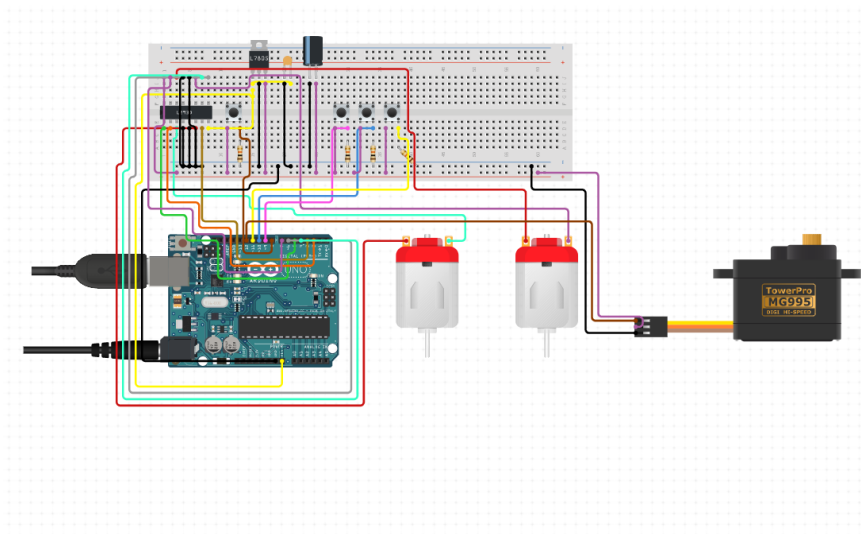


Figure A.3: Circuit of the control section

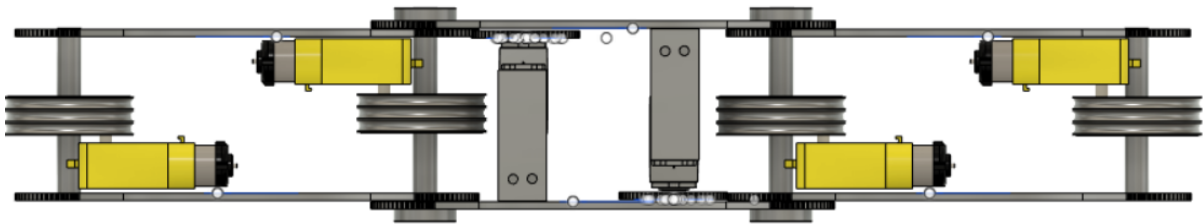
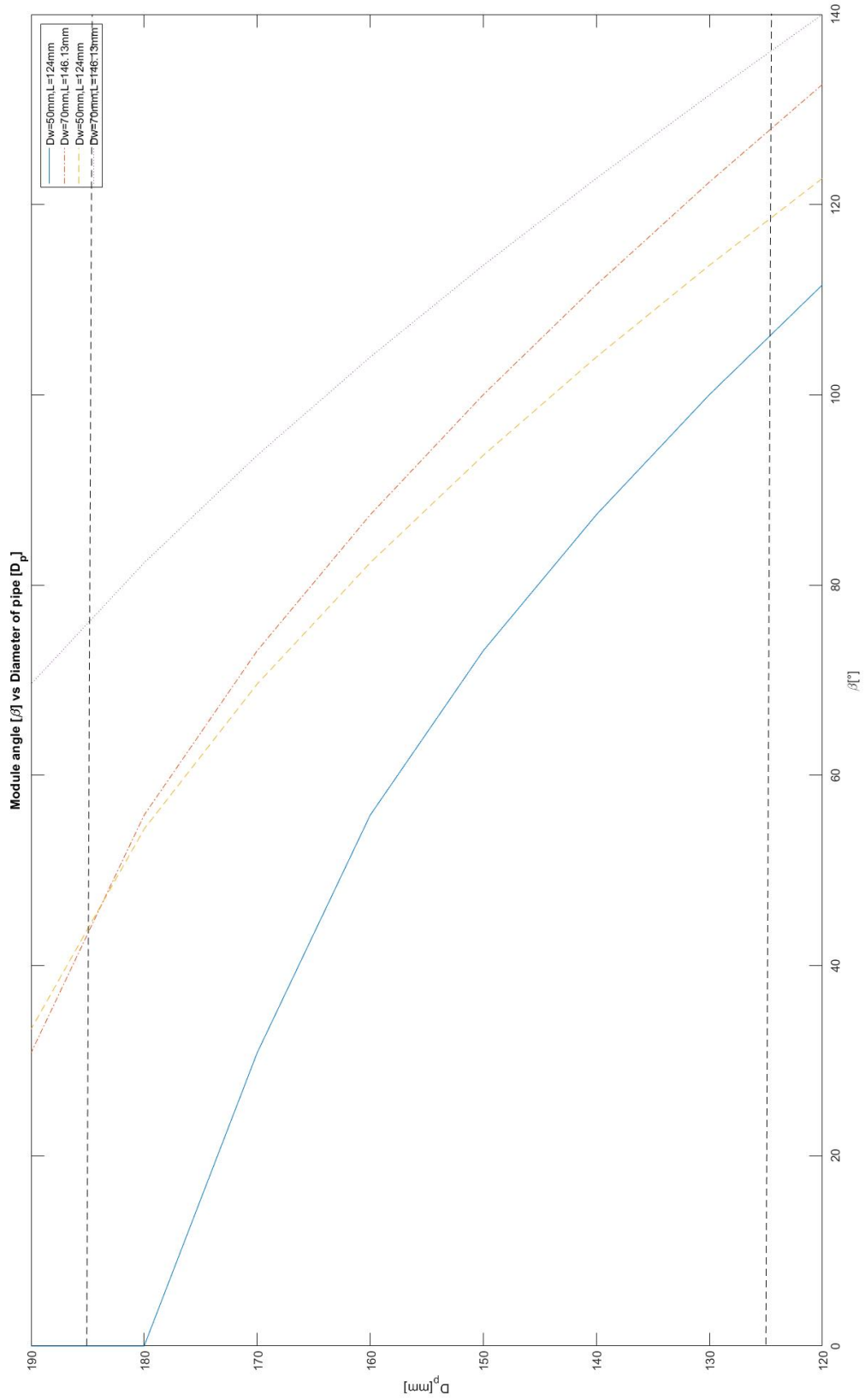


Figure A.4: Top view for 3 modules



Figure A.5: Final design



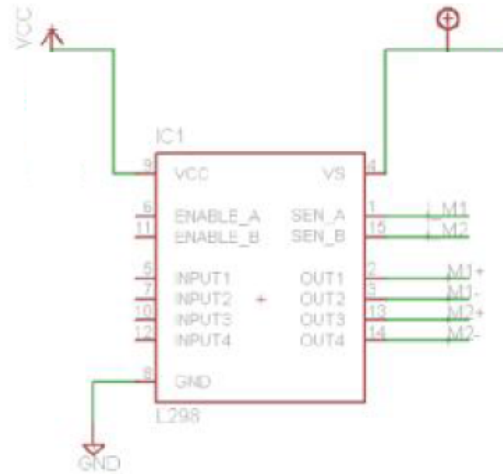


Figure A.7: L293d motordriver Instruments (2016)

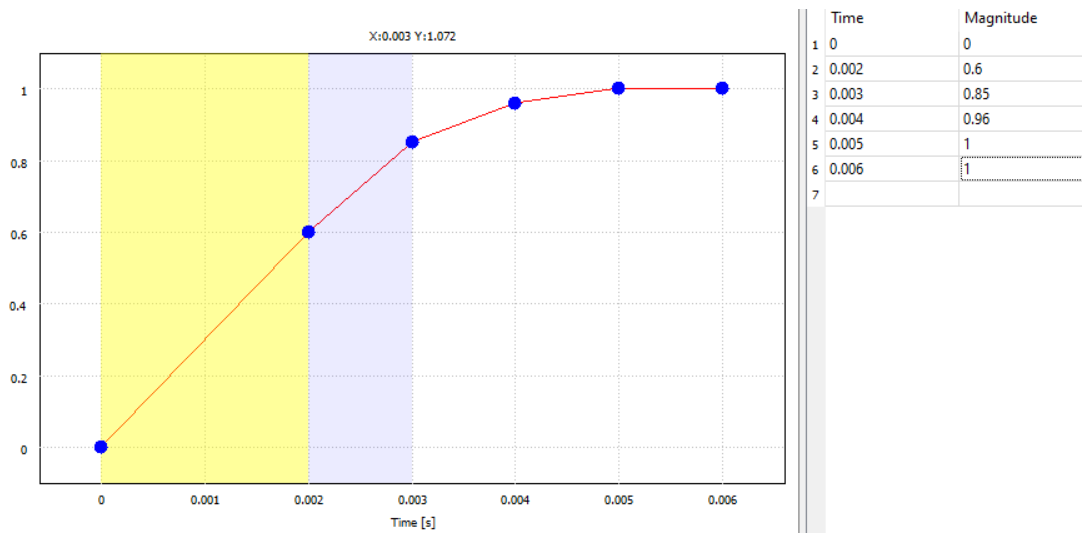


Figure A.8: Simulation setup of force magnitudes

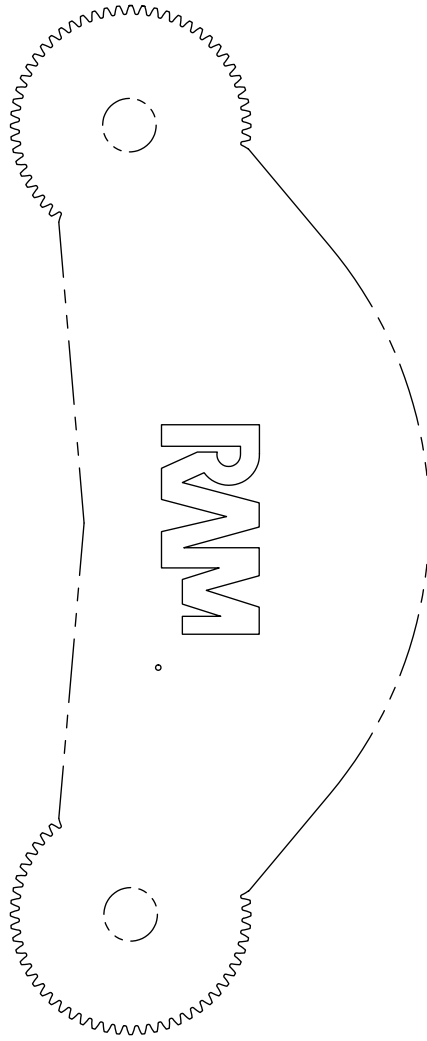
Dw	Dp	Dx	l	r[m]	Ftr (30 deg	Fc	T[Nm]	T/2
50	120	70	75.77398	0.029012			0.251342	0.125671
50	130	80	86.59883	0.033157			0.287247	0.143624
50	140	90	97.42368	0.037301			0.323153	0.161577
50	150	100	108.2485	0.041446			0.359059	0.17953
50	160	110	119.0734	0.04559			0.394965	0.197483
50	170	120	129.8982	0.049735	8.663366	28.87789	0.430871	0.215436
50	180	130	140.7231	0.053879			0.466777	0.233389
50	190	140	151.548	0.058024			0.502683	0.251342
50	200	150	162.3728	0.062169			0.538589	0.269294
50	210	160	173.1977	0.066313			0.574495	0.287247
50	220	170	184.0225	0.070458			0.610401	0.3052

Figure A.9: Calculations sample for $\beta = 45$ deg

B Appendix2

B.1 Designs 2D sketches

Figure B.1: 2D laser cut model for Side Module



Dept.	Technical reference	Created by Yash Mirwani	11/16/2019	Approved by	
		Document type		Document status	
		Title		DWG No.	
		New gears on side module for bigger pipes > 16.5cm/2 entries		Rev.	Date of issue
					Sheet
					1/1

Figure B.2: 2D laser cut model for axis mount

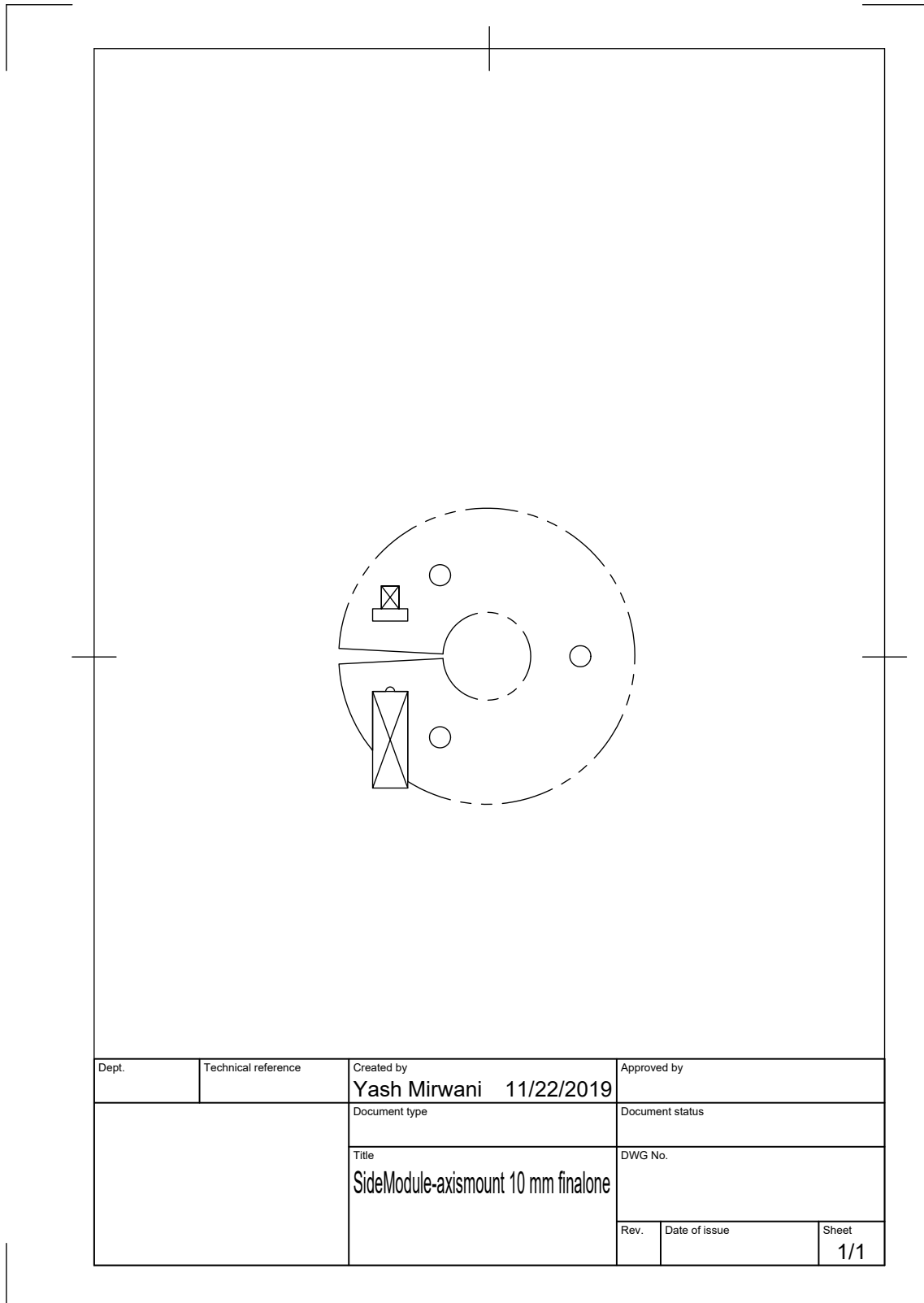
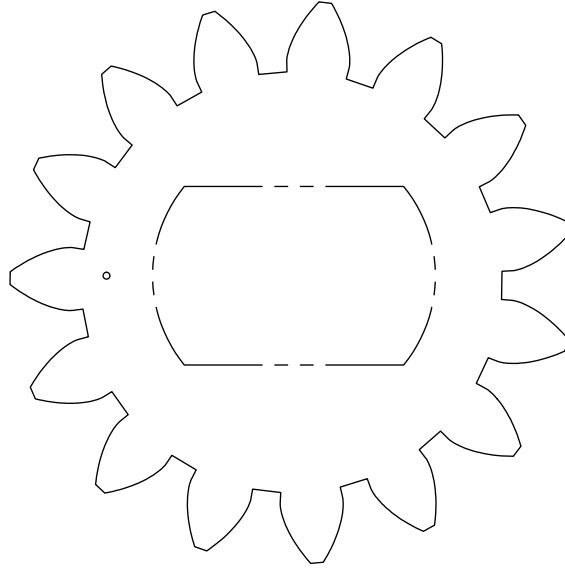


Figure B.3: 2D laser cut model of gears for DC geared motor



Dept.	Technical reference	Created by Yash Mirwani	11/22/2019	Approved by	
		Document type		Document status	
		Title	Gear15teethNewDimensions	DWG No.	
				Rev.	Date of issue
					Sheet
					1/1

Figure B.4: 2D model sketch of mounting of servomotor

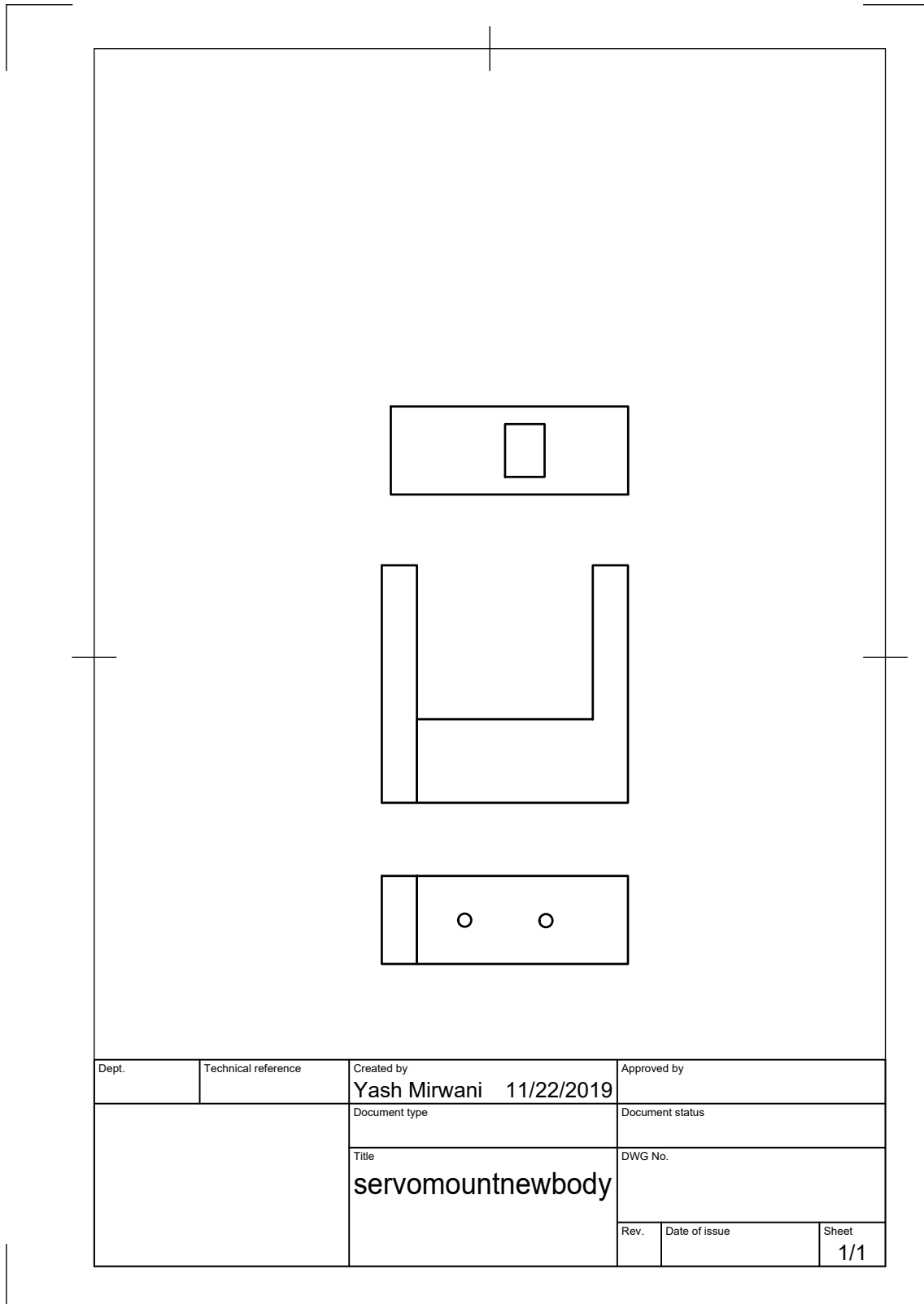


Figure B.5: 2D model sketch of wheels

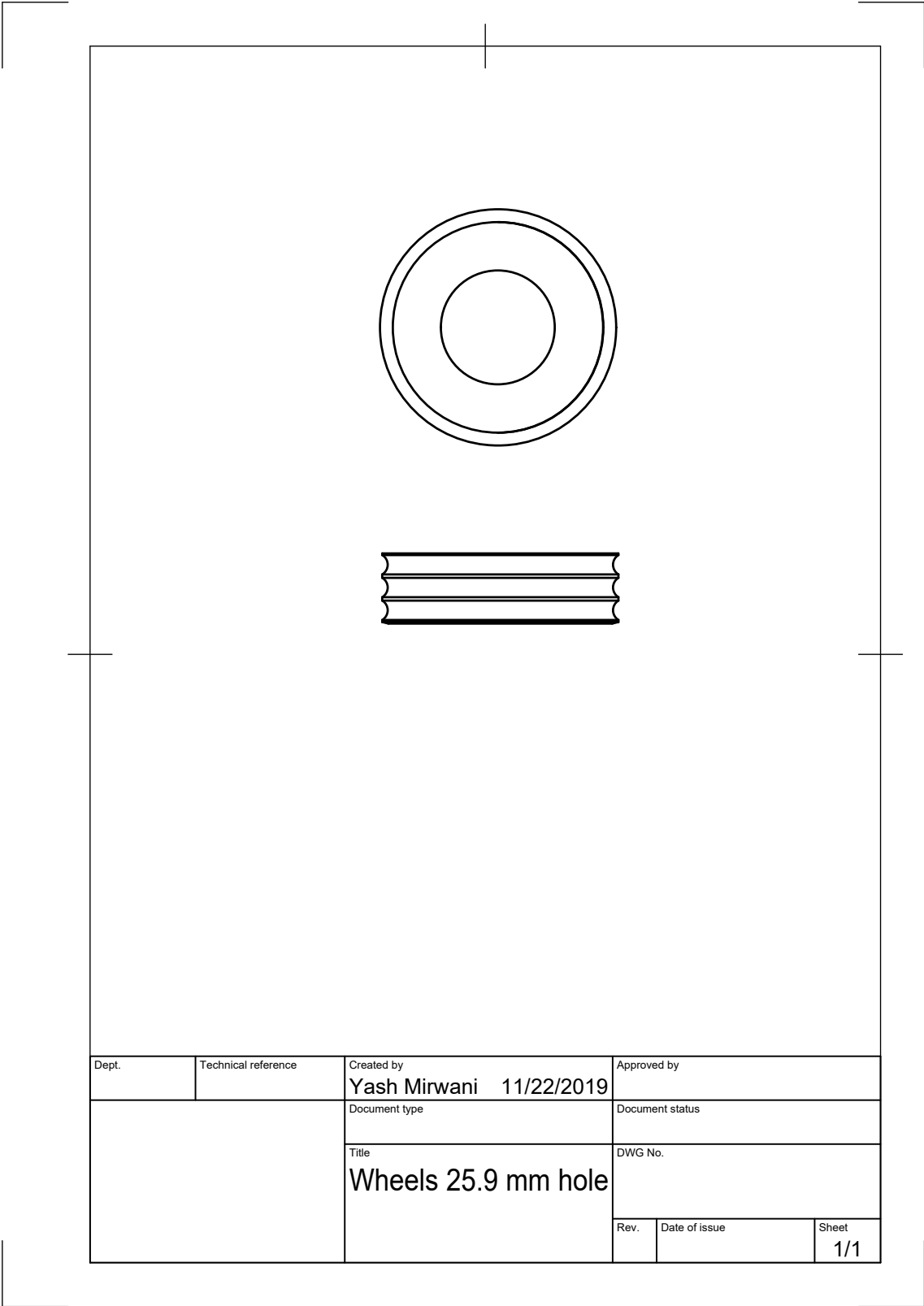


Figure B.6: 2D laser cut model for internal gears for wheel module

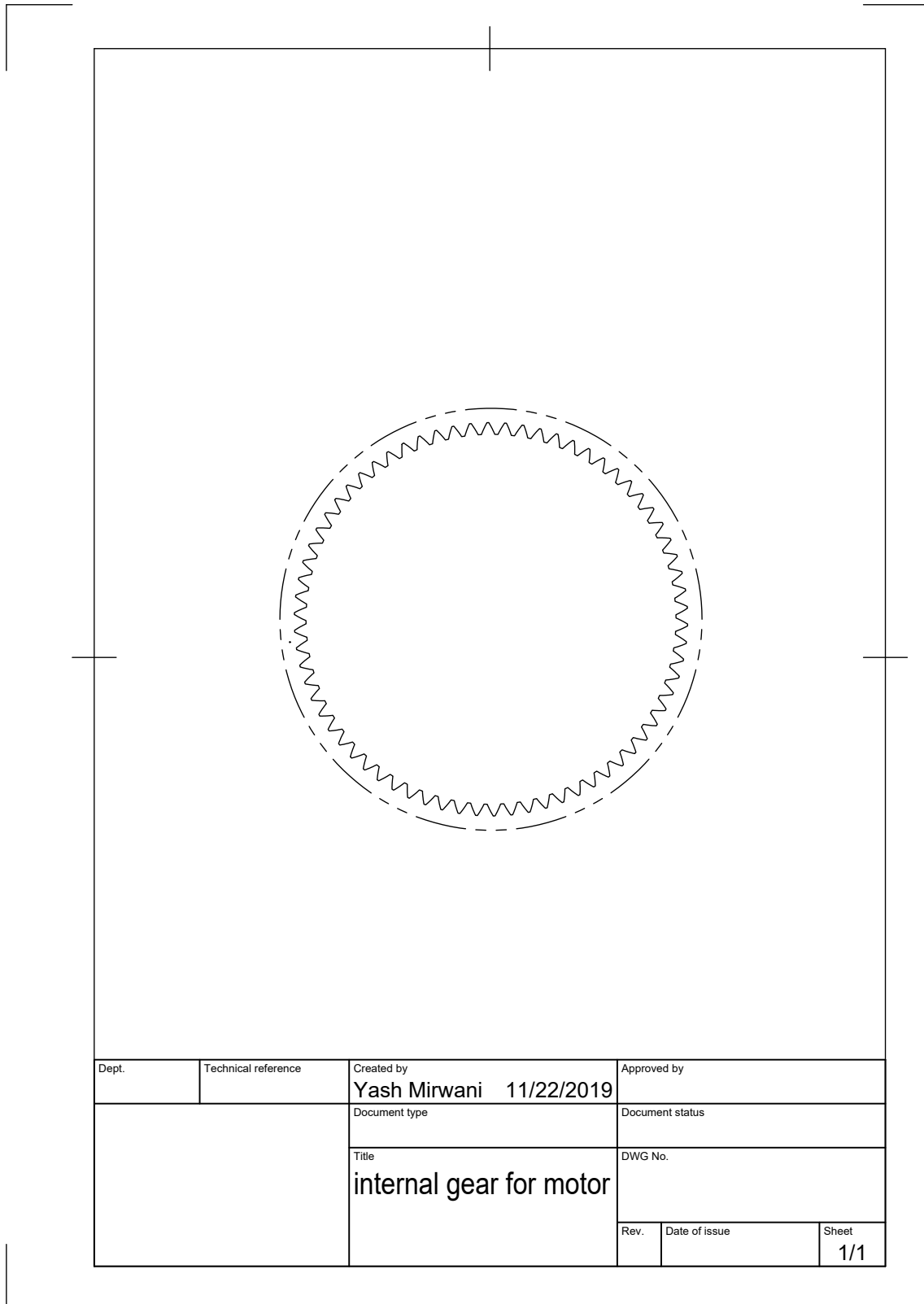


Figure B.7: 2D laser cut model of gears for servomotor

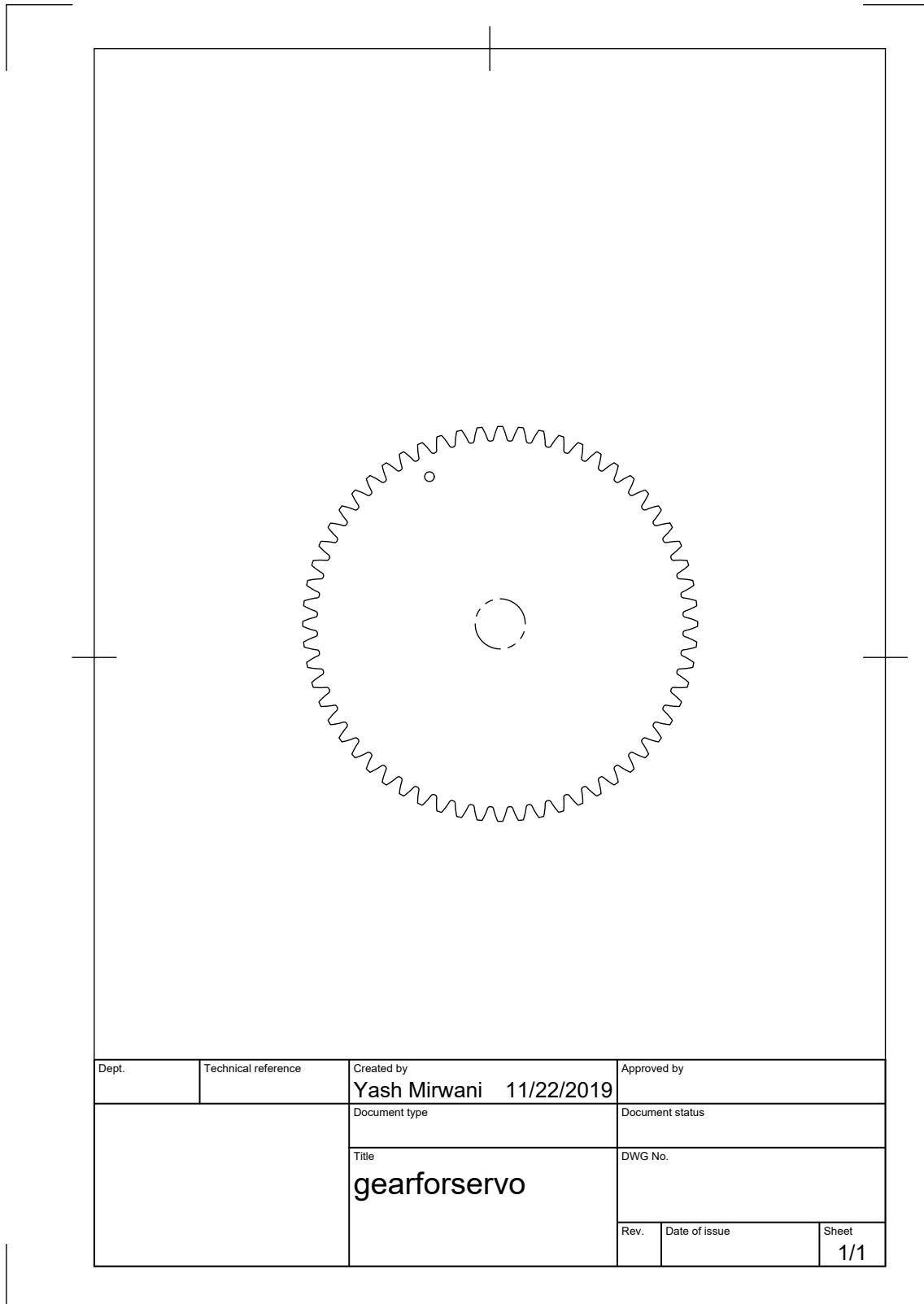
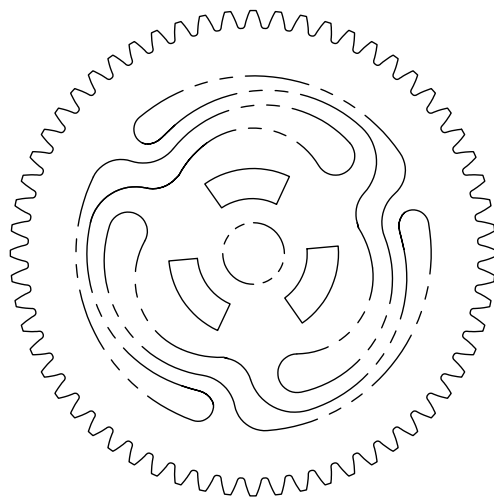


Figure B.8: 2D laser cut model- Spring gear



Dept.	Technical reference	Created by Yash Mirwani 11/22/2019	Approved by	
		Document type	Document status	
		Title SpringGearscaledFinalT1	DWG No.	
		Rev.	Date of issue	Sheet 1/1

Bibliography

- (2019), *MATLAB 9.7 (2019a)*, The Mathworks, Inc., Natick, Massachusetts.
- Aasvik, M. (2015), Basic Static Stress Simulation in Fusion 360.
<https://www.norwegiancreations.com/2016/07/basic-static-stress-simulation-in-fusion-360/>
- Borgerink, D., D. Brouwer, J. Stegenga and S. Stramigioli (2016), Kinematic Design Method for Rail-Guided Robotic Arms, *Journal of Mechanisms and Robotics*, **vol. 9**, doi:10.1115/1.4035187.
- Braun, J. (2016), Formulae handbook- Maxon academy.
<https://innodrive.ru/wp-content/uploads/docs/info.pdf>
- Ceccarelli, M. (2003), Low-Cost Robots for Research and Teaching Activities.
- Dertien, E. (2006), System specifications for pirate, *Edwin Dertien, Control laboratory, University of Twente, the Netherlands*.
- Fitzner, I., Y. Sun, V. Sachdeva and S. Revzen (2017), Rapidly Prototyping Robots: Using Plates and Reinforced Flexures, **vol. 24**, no.1, pp. 41–47, ISSN 1558-223X, doi:10.1109/MRA.2016.2639058.
- Global, N. (2017), Bearing Load Calculation.
https://www.ntnglobal.com/en/products/catalog/pdf/2202E_a04.pdf
- Instruments, T. (2016), L293x Quadruple Half-H Drivers.
<http://www.ti.com/lit/ds/symlink/l293.pdf>
- Pulles, C., E. Dertien, P. J and R. Nispeling (2008), Pirate, the development of an autonomous gas distribution system inspection robot, *Journal of Membrane Science - J MEMBRANE SCI*.
- Rubenstein, M., C. Ahler, N. Hoff, A. Cabrera and R. Nagpal (2014), Kilobot: A low cost robot with scalable operations designed for collective behaviors, *Robotics and Autonomous Systems*, **vol. 62**, p. 966–975, doi:10.1016/j.robot.2013.08.006.
- Stramigioli, S. and N. Botteghi (2018), SMART TOOLING- Automation in the process industry for safer, cheaper, cleaner, and more efficient maintenance.
<https://www.ram.ewi.utwente.nl/research/projects/smart-tooling>